OPEN

Citation: Oncogenesis (2013) **2**, e66; doi:10.1038/oncsis.2013.29

www.nature.com/oncsis

ORIGINAL ARTICLE

Gremlin-1 associates with fibrillin microfibrils *in vivo* and regulates mesothelioma cell survival through transcription factor slug

JA Tamminen[1,2], V Parviainen[2], M Rönty[3,4], AP Wohl[5], L Murray[1,2], S Joenväärä[2], M Varjosalo[6], O Leppäranta[7], O Ritvos[3,8], G Sengle[5], R Renkonen[2,3], M Myllärniemi[7] and K Koli[1,2]

Malignant mesothelioma is a form of cancer that is highly resistant to conventional cancer therapy for which no major therapeutic advances have been introduced. Here, we identify gremlin-1, a known bone morphogenetic protein inhibitor crucial for embryonic development, as a potential therapeutic target for mesothelioma. We found high expression levels of gremlin-1 in the mesothelioma tumor tissue, as well as in primary mesothelioma cells cultured from pleural effusion samples. Downregulation of gremlin-1 expression by siRNA-mediated silencing in a mesothelioma cell line inhibited cell proliferation. This was associated with downregulation of the transcription factor slug as well as mesenchymal proteins linked to cancer epithelial-to-mesenchymal transition. Further, resistance to paclitaxel-induced cell death was associated with high gremlin-1 and slug expression. Treatment of gremlin-1-silenced mesothelioma cells with paclitaxel or pemetrexed resulted in efficient loss of cell survival. Finally, our data suggest that concomitant upregulation of fibrillin-2 in mesothelioma provides a mechanism for extracellular localization of gremlin-1 to the tumor microenvironment. This was supported by the demonstration of interactions between gremlin-1, and fibrillin-1 and -2 peptides as well as by colocalization of gremlin-1 to fibrillin microfibrils in cells and tumor tissue samples. Our data suggest that gremlin-1 is also a potential target for overcoming drug resistance in mesothelioma.

Oncogenesis (2013) **2,** e66; doi:10.1038/oncsis.2013.29; published online 26 August 2013

Subject Categories: Molecular oncology

Keywords: gremlin; fibrillin; mesothelioma; EMT; slug

INTRODUCTION

Malignant mesothelioma is an aggressive tumor, which originates from the mesothelial surface cells lining the serous body cavities such as the pleura, peritoneum or pericardium.[1] Mesothelioma is strongly linked to asbestos exposure, and it may take several decades to develop after initial exposure.[2] Because of the long latency, the incidence of mesothelioma will increase in the near future worldwide.[3,4] Mesothelioma is resistant to chemo- and radiotherapy, leading to poor prognosis for patients suffering from this malignancy.[4] New markers for screening and monitoring the disease and in particular new drug targets are needed.

Cancer progression is associated with a re-expression of developmental programs, which contribute to the proliferative and invasive properties of tumor cells.[5,6] Gremlin-1 is a cysteine knot protein, which belongs to the DAN family of bone morphogenetic protein (BMP) antagonists. Gremlin-1 can bind to and inhibit the functions of BMP-2, -4 and -7.[7,8] These three BMP isoforms are targeted to fibrillin microfibrils, suggesting extracellular regulation of bioavailability.[9] Gremlin-1-mediated BMP antagonism is crucial for mouse lung and kidney development.[10] In adult mouse and human tissues gremlin-1 expression is low. Originally, gremlin-1 was identified as a gene downregulated in *v-mos*-transformed fibroblasts and therefore called Drm.[11] However, recent studies suggest the overexpression of gremlin-1 in epithelial cancers including lung carcinomas.[12,13]

The role of gremlin-1 in cancer has remained largely unclear. As our preliminary results suggested an upregulation of gremlin in mesothelioma tissue, we set out to find molecular interactions of gremlin and study the biological function of gremlin in mesothelioma.

RESULTS

Gremlin-1 interacts with fibrillin-1 and -2

A search for new gremlin interacting proteins was carried out using systematic affinity purification coupled with mass spectrometry identification (AP-MS). We used the well-characterized Flip-In-HEK293 cell system to produce C-terminally tagged gremlin-1 and a standardized workflow for the purification of protein complexes from cell lysates[14] (Figure 1a). A low tetracycline concentration (25 ng/ml) was selected for gremlin-1 induction (Figure 1b). Immunoblotting analyses after different affinity purification steps suggested that gremlin was well recovered (Figure 1c).

In order to characterize the interactome of gremlin-1, immunopurified proteins were identified using mass spectrometry. Proteins

[1]Research Programs Unit, Translational Cancer Biology, University of Helsinki, Helsinki, Finland; [2]Transplantation Laboratory, Haartman Institute, University of Helsinki, Helsinki, Finland; [3]Helsinki University Central Hospital and Hospital Laboratory, Helsinki, Finland; [4]Department of Pathology, University of Helsinki, Helsinki, Finland; [5]Center for Biochemistry, Medical Faculty, University of Cologne, Cologne, Germany; [6]Institute of Biotechnology, University of Helsinki, Helsinki, Finland; [7]Division of Pulmonary Medicine, Department of Medicine, University of Helsinki, Helsinki, Finland and [8]Department of Bacteriology and Immunology, University of Helsinki, Helsinki, Finland. Correspondence: Dr K Koli, University of Helsinki, Biomedicum/B502a1, PO Box 63, Haartmaninkatu 8, Helsinki 00014, Finland.
E-mail: katri.koli@helsinki.fi
Received 10 July 2013; accepted 16 July 2013

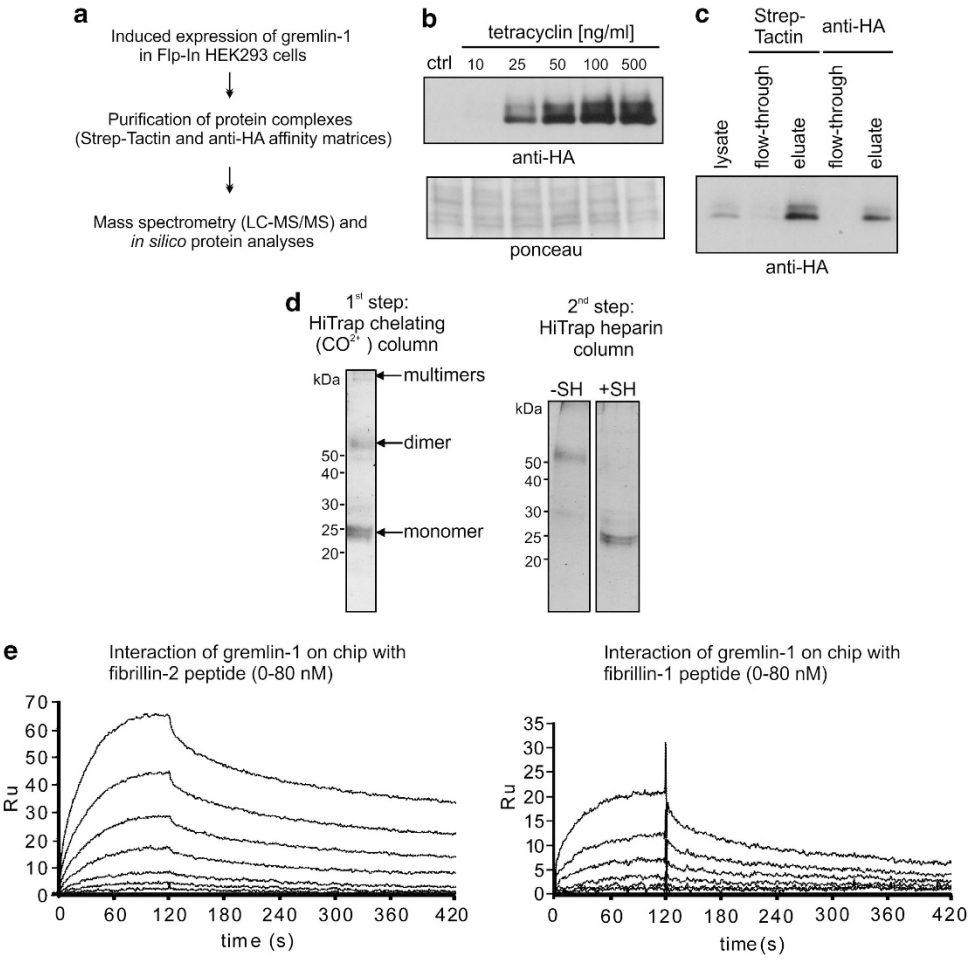

Figure 1. Gremlin-1 interacts with fibrillin-1 and -2. (**a**) Gremlin-1 protein interaction screen outline. (**b**) Flip-In HEK293/gremlin-1 cells were treated with increasing concentrations of tetracycline for 24 h followed by immunoblotting analyses using anti-HA antibodies. Ponceau staining of proteins indicates equal loading. (**c**) Immunoblotting analyses of gremlin-1, using anti-HA antibodies, after Strep-tactin and anti-HA affinity purification steps. (**d**) Purification of gremlin-1 from conditioned media of stably transfected HEK293 cells. After elution from a $CoCl_2$-loaded HiTrap column using a C-terminally placed His_6-affinity-tag protein, bands corresponding to monomeric, dimeric and multimeric gremlin-1 were detected via SDS–PAGE followed by Coomassie staining. A subsequent second purification step via a HiTrap heparin column yielded mostly dimeric gremlin-1, which shifted to the position of monomeric gremlin under reducing conditions (+SH). (**e**) Interaction studies between gremlin-1 and N-terminal peptides of fibrillin-1 and -2 using a surface plasmon resonance technology. Gremlin-1 was immobilized on a sensor chip and fibrillin-1 and -2 peptides in a concentration range from 80 to 0 nM were flown over as analytes. Affinity constants (K_d) for both interactions were about 10 nM (Table 1), indicating a high affinity interaction between gremlin-1 and the main building blocks of fibrillin microfibrils.

were first digested using trypsin and then fractionated with reverse-phase chromatography online using a mass spectrometer. The resulting peptide spectra were identified with two different search engines. A total of 12 proteins were identified to interact with gremlin-1 in three replicate experiments and with both search engines. The interaction data were filtered using a protein list (data not shown) of 377 unspecific binding proteins acquired using Flip-In-HEK293 cell line transfected with the affinity tag containing plasmid. The final filtered list contained four proteins: cytokeratin-9 (Swiss-Prot: P35527), fibrillin-2 (Swiss-Prot: P35556), cytokeratin-2a (Swiss-Prot: P35908) and APOBEC1-binding protein 2 (Swiss-Prot: Q9UBS4). Fibrillin-2 was identified in all three replicate experiments and with both search engines, which improves the confidence of the identification. In addition, fibrillin-2 was identified with up to three distinct and good scoring peptides in two of the replicates further validating the interaction of fibrillin-2 and gremlin-1. Fibrillins are constituents of extracellular microfibrils and have a role in elastin assembly.[15] They also sequester and regulate the bioavailability of growth factors such as BMP isoforms.[9]

Table 1. Surface plasmon resonance affinity data for tested interactions between gremlin-1 and fibrillin-1 and -2 N-terminal peptides

Interaction (ligand/analyte)	k_{on} *(1/M*s)/*k_{off} *(1/s)*	K_d *(nM)*
gremlin-1 dimer/ fibrillin-2 (rF86)	2.41×10^5/ 2.18×10^{-3}	9.05
gremlin-1 dimer/ fibrillin-1 (rF11)	1.92×10^5/ 1.45×10^{-3}	7.55

In order to confirm our findings, we tested direct interactions between purified gremlin-1 and recombinant N-terminal peptides of fibrillin-1 and -2 in protein–protein interaction assays using surface plasmon resonance technology. When purified gremlin-1 (Figure 1d) was used as a ligand immobilized on the sensor chip surface and N-terminal fibrillin were flown over as analytes direct interactions with molecular affinities in the low nanomolar range (Table 1) could be measured (Figure 1e). This suggests a high

molecular interaction between gremlin-1 and the two main building blocks of fibrillin microfibrils.

Gremlin-1 and fibrillin-2 are overexpressed in the mesothelioma tumor tissue and colocalize *in vivo*

To analyze whether gremlin-1 and fibrillins are coexpressed *in vivo*, tissue biopsies from mesothelioma patients included in this study were stained with specific antibodies. We had previously shown low levels of gremlin expression in the normal lung.[16] Here, we detected low expression of gremlin in normal mesothelial cells (Figure 2a). Gremlin-1 staining was, however, detected in non-malignant, reactive mesothelial cells in control samples (pneumothorax). Intense gremlin-1 immunoreactivity was observed in all mesothelioma samples ($n = 6$). Fibrillin-2 immunoreactivity was shown in a strikingly similar staining pattern as observed for gremlin-1 in these tumor samples, suggesting concomitant upregulation of these developmental genes in mesothelioma. Some fibrillin-2 staining was detectable also in non-malignant reactive mesothelium. Calretinin and WT1 (Wilm's tumor 1) are diagnostic markers for mesothelioma and were used here to identify the tumor tissue. Analyses of serial tissue sections suggested that gremlin-1 and fibrillin-2 staining localizes to calretinin-positive and -negative tumor areas (Figure 2b). Some WT-1 positivity, however, was observed in calretinin-negative areas, which represent sarcomatoid part of the tumor with more diffuse growth properties. Fibrillin-1 staining was negative in 5/6 mesothelioma and in control pleura samples. Only one mesothelioma sample showed fibrillin-1 immunoreactivity, which was specifically detected in stromal-like areas (not shown).

We analyzed colocalization of gremlin-1 with fibrillin-2 in tumor tissue using the proximity ligation assay. Intensive colocalization signals were observed for gremlin-1 and fibrillin-2 throughout the tumor tissues, suggesting that they localize to similar structures *in vivo* (Figure 3).

Primary human mesothelioma cells express high levels of gremlin-1 and fibrillin-2

Primary cells were cultured from mesothelioma patients' pleural effusion samples (JP1-5). Cells were characterized by immunofluorescence staining using mesothelial markers calretinin and cytokeratin (CK)-7 as well as vimentin, which is commonly expressed by tumor cells. Majority of the cells were calretinin- and/or CK-7 positive and stained also for vimentin (Figure 4a). This suggests that the cells, which were able to proliferate, were mainly primary tumor cells. Gremlin-1 mRNA expression levels were high in these primary cells compared with Met5A cells, which are immortalized but non-tumorigenic mesothelial cells (Figure 4b). Further, the mRNA expression levels of fibrillin-1 and -2 were high in these cells (Figure 4b). The results show that primary mesothelioma cells can be cultured from pleural effusion samples and that the cells retain the phenotypic expression of these developmental genes.

Gremlin-1 is known to inhibit the functions of BMP-2, -4 and to some extent also BMP-7.[7,8] Therefore, the expression levels of these BMP isoforms were analyzed in primary mesothelioma cells.

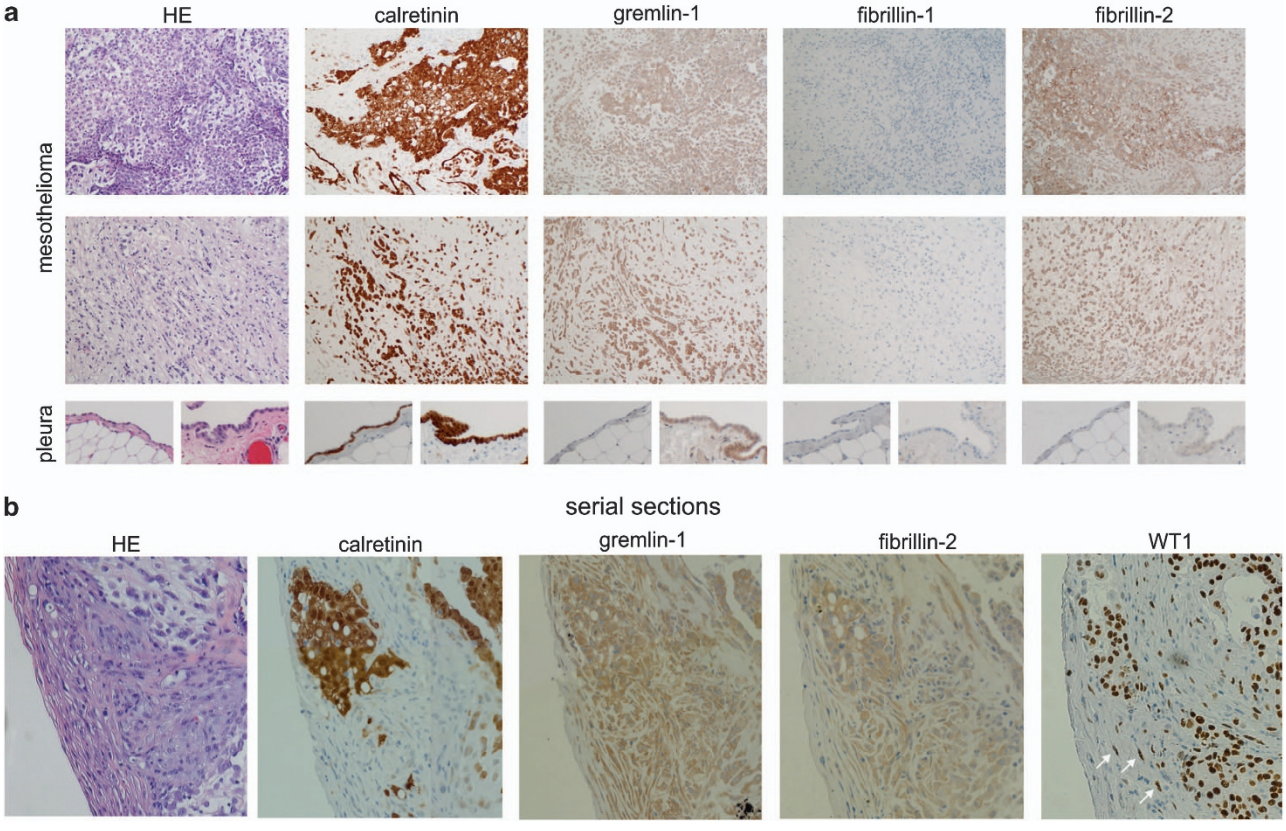

Figure 2. Overexpression of gremlin-1 and fibrillin-2 in mesothelioma. (**a**) Immunohistochemical staining of mesothelioma and control pleura samples using calretinin, gremlin-1, fibrillin-1 and fibrillin-2 antibodies. Hematoxylin and eosin (HE) staining is shown on the left. Abundant gremlin-1 and fibrillin-2 immunoreactivity is observed in both calretinin-negative and -positive tumor areas. Normal mesothelium (pleura, left panel) shows very low levels of staining, whereas reactive normal mesothelium (pleura, right panel) shows faint fibrillin-2 and moderate gremlin-1 staining. (**b**) Immunohistochemical staining of serial mesothelioma sections suggests similar staining patterns for gremlin-1 and fibrillin-2. Staining was observed also in calretinin-negative stromal-like areas, which contained isolated Wilms' tumor protein (WT1)-positive tumor cells (white arrows).

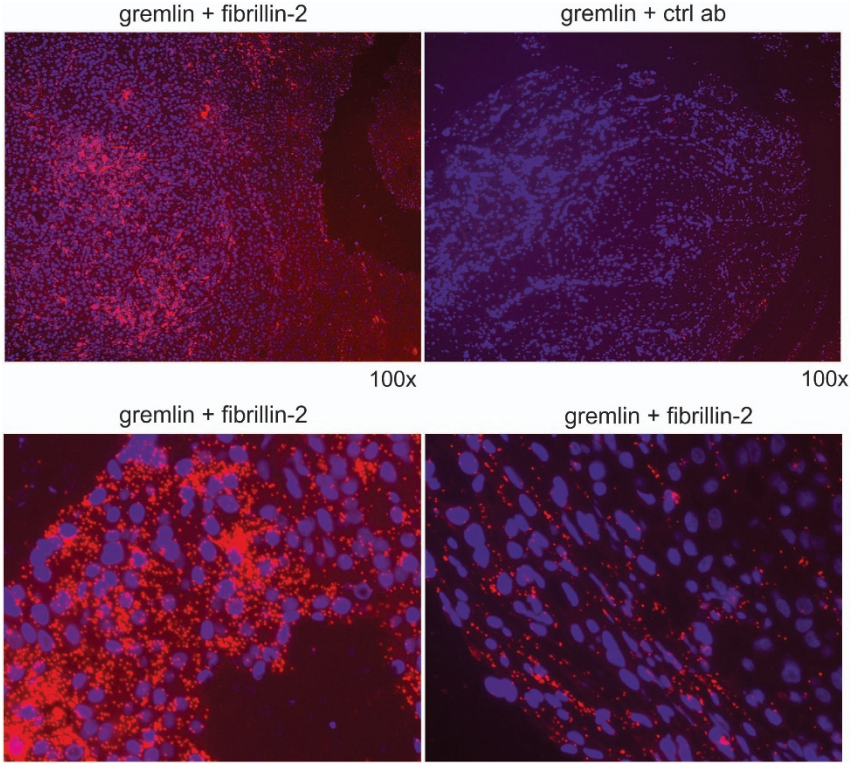

Figure 3. Colocalization analyses of gremlin-1 with fibrillin-2 in mesothelioma tumor tissue. Proximity ligation assay was used to detect colocalization of gremlin-1 with fibrillin-2 in mesothelioma tumor tissue. Positive colocalization signals (red dots) were abundant throughout the tumor tissue. Negative control with gremlin antibody plus mouse isotype control is shown on the upper right panel.

Interestingly, abundant expression of BMP-2 was observed (Figure 4b), whereas BMP-4 levels were comparable and BMP-7 levels only slightly higher compared with Met5A cells (not shown).

The expression patterns of gremlin-1, fibrillins and BMP-2 were also analyzed in four established mesothelioma cell lines (211H, H28, H2452 and H2052). Only one of these cell lines, H2052, resembled primary mesothelioma cells and expressed high levels of gremlin-1, fibrillin-2 and BMP-2 (Figure 4c). Therefore, this cell line was chosen for further mechanistic studies.

Gremlin-1 associates with fibrillin-1 in cultured mesothelioma cells

Mesothelioma cells were cultured for 1 week and then analyzed by immunofluorescence staining using antibodies specific for gremlin-1 or fibrillins. Although expressed at the mRNA level, fibrillin-2 protein was not detected in any of the cultured mesothelioma cells analyzed at this time point (not shown), which may reflect late extracellular matrix (ECM) deposition *in vitro*. Primary mesothelioma cells and H2052 cells *in vitro* also expressed fibrillin-1 mRNA, and this was reflected in the staining pattern showing fibrillar staining for fibrillin-1 and gremlin-1 (Figure 5a). No staining was observed in H2452 cells. Double immunofluorescence labeling suggested colocalization and targeting of gremlin-1 into fibrillin-1 containing microfibrils *in vitro*. H2052 cells transfected with fibrillin-1-specific siRNA showed reduced mRNA expression levels (Figure 5b) and significantly reduced fibrillin-1 staining, indicating efficient silencing of protein expression (Figure 5c). This led to reduced deposition of gremlin into fibrillar structures suggesting that extracellular targeting of gremlin is dependent on fibrillins.

Gremlin-1 silencing severely impairs mesothelioma cell growth and survival

To investigate the role of gremlin-1 in mesothelioma cell growth, H2052 cells were transfected with gremlin-specific siRNAs. Efficient silencing of gremlin-1 expression was observed at mRNA and protein levels (Figures 6a and b). Cell proliferation was assayed by counting cells 1–5 days after transfection. Two independent siRNAs targeted against gremlin-1 were observed to significantly decrease the number of cells at all time points (Figure 6c). This suggests that H2052 cell proliferation is dependent on gremlin expression.

To determine whether lack of gremlin induces apoptosis, H2052 cells were cultured on coverslips, transfected with siRNAs and analyzed with TUNEL assay 3 days after transfection (Figure 6d). Hardly any TUNEL-positive cells were detected in control or gremlin siRNA-transfected cells. DAPI staining also showed intact nuclei in both groups. These results suggest that although lack of gremlin impaired cell proliferation, it did not induce apoptosis.

Cellular signaling pathway activities are altered in gremlin-1-silenced cells

Changes in BMP signaling activity were analyzed. Gremlin-1 silencing increased BMP-dependent reporter activity in H2052 cells (Figure 7a) as well as the expression of a BMP target gene *Id1* (inhibitor of differentiation/DNA binding 1, Figure 7b), suggesting that endogenous gremlin-1 regulates BMP activity negatively. Further, Id1 expression was found significantly reduced in primary mesothelioma cells compared with Met5A cells (Figure 7c).

To further investigate cellular signaling pathways regulated by gremlin, we analyzed alteration in phospho-kinase levels using a commercial array (see Materials and methods). H2052 cells were found to have high basal level of phospho-Akt (S473), which was not altered in gremlin-1-silenced cells (Figures 7d–f). However, phosphorylation of the Akt substrate and regulator of mTOR signaling, PRAS40 (T246), was increased. Erk1/2 phosphorylation was also significantly increased in gremlin-1-silenced cells (g). Further, increased levels of p53 phosphorylation (S46 and S392)

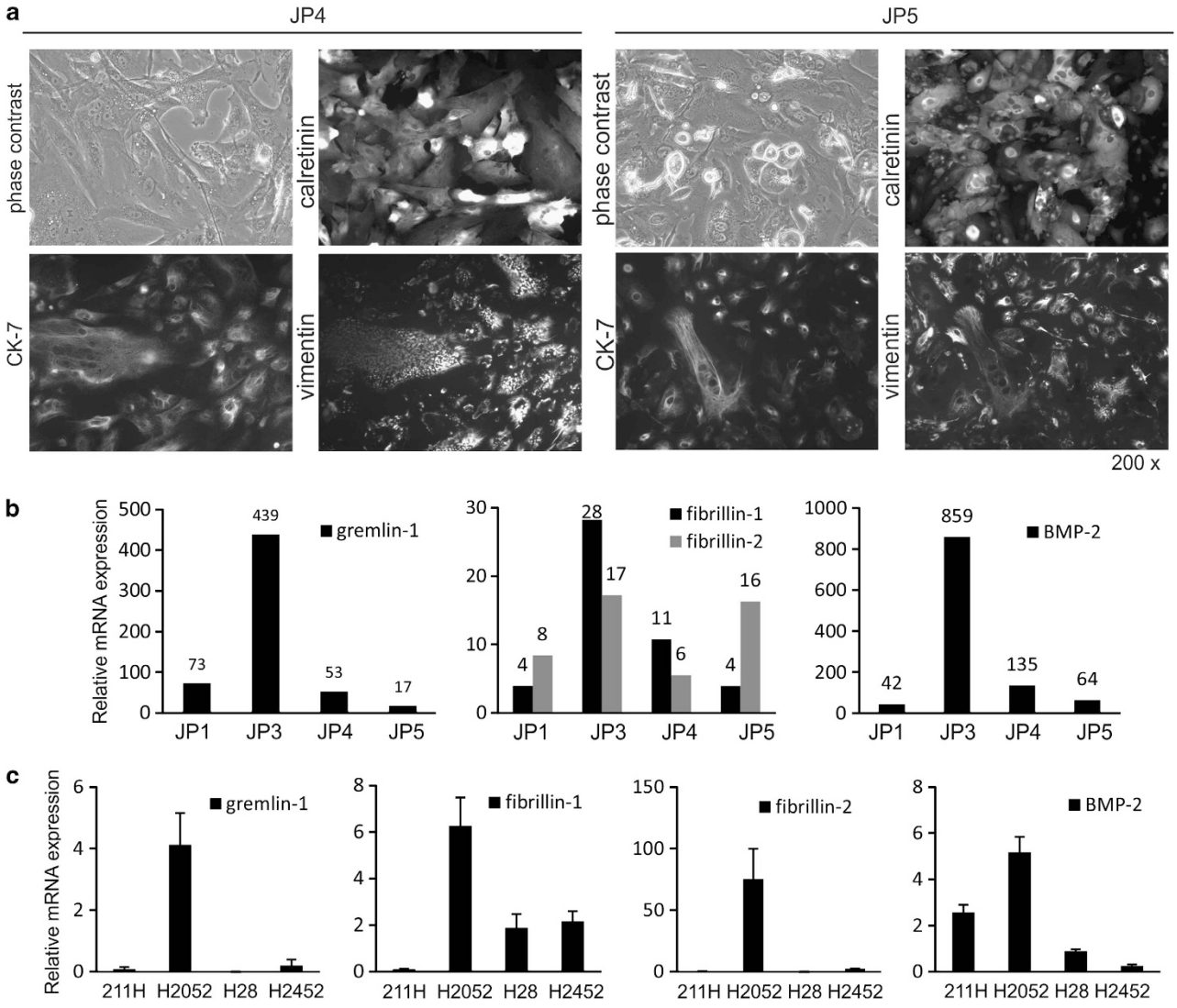

Figure 4. Primary mesothelioma cells express high levels of gremlin-1. Primary mesothelioma cells (JP cells) were isolated from pleural effusion samples. (**a**) Immunofluorescence staining suggests that the cells were positive for the mesothelial marker calretinin. Co-staining with cytokeratine (CK)-7 and vimentin antibodies suggests that the tumor cells co-express these marker proteins. (**b**) Primary mesothelioma cells were analyzed for gremlin-1, fibrillin-1 and -2 and BMP-2 mRNA expression by quantitative RT–PCR. The levels were normalized to the expression levels of TATA-binding protein and are expressed relative to the expression levels in Met5A cells (immortalized, non-tumorigenic mesothelial cells), which were set to 1. (**c**) Established mesothelioma cell lines were analyzed for gremlin-1, fibrillin-1 and -2 and BMP-2 mRNA expression by quantitative RT–PCR. The error bars represent s.d. ($n = 2$).

were reflected in increased mRNA expression levels of p21 (Cip1/Waf1) in H2052 cells (Figure 7h). In agreement, overexpression of gremlin-1 in H2052 and H28 cells decreased p21 expression levels (Figure 7i).

Gremlin-1 expression is associated with EMT phenotype and chemoresistance

Gremlin-1 expression has been linked to EMT processes. Therefore, we determined whether mesothelioma cells with high gremlin levels express transcription factors snail and slug, which are transcriptional repressors of E-cadherin and induce EMT.[17] Whereas the mRNA expression levels of snail were comparable in mesothelioma cells and Met5A cells, slug expression levels were high in primary mesothelioma cells (Figure 8a). Slug expression in mesothelioma tumor samples was analyzed using immunohistochemical staining (Figures 8b and c). All of the analyzed tumor samples ($n = 6$) were positive for slug. Mesothelioma tumors exhibited mostly diffuse and granular cytoplasmic staining, but also nuclear staining was detected in certain tumor areas. Slug staining localized to gremlin-positive areas and was detected also in calretinin-negative areas.

Similar to primary mesothelioma cells H2052 cells, which express high levels of gremlin-1, exhibited high slug expression (Figure 8d). Conversely, Met5A and H2452 cells showed very low levels of slug mRNA expression consistent with low gremlin-1 expression levels. Slug protein levels also showed a dramatic difference between H2052 and H2452 cells (Figure 8d). Silencing of gremlin-1 by siRNA transfection significantly reduced slug mRNA and protein expressions in H2052 cells (Figure 8e and i). Similar results were also obtained with primary mesothelioma cells (Figure 8f). Further, overexpression of gremlin-1 in H28 cells led to increased slug mRNA expression (Figure 8g). The mRNA and especially protein expression levels of mesenchymal proteins, N-cadherin, vimentin and α-smooth muscle actin were significantly downregulated in gremlin-1-silenced H2052 cells (Figures

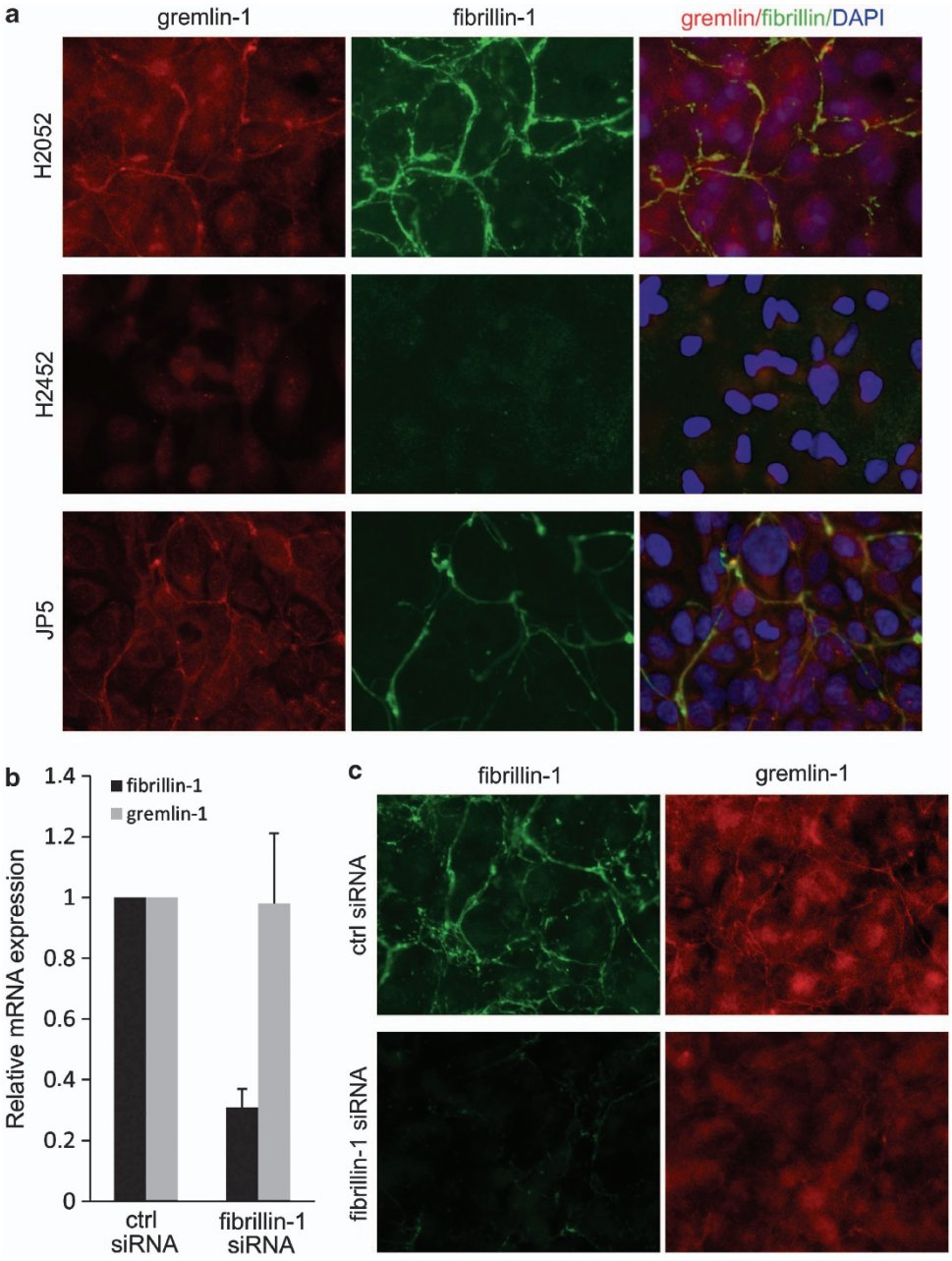

Figure 5. Gremlin-1 and fibrillin-1 co-localize in mesothelioma cell ECM *in vitro*. (**a**) Mesothelioma cell lines (H2052 and H2452) and primary mesothelioma cells (JP5) were co-stained for gremlin-1 and fibrillin-1 and analyzed using immunofluorescence microscopy. A fibrillar staining pattern was observed in H2052 and JP5 cells. (**b**) In control (ctrl) and fibrillin-1 siRNA-transfected H2052 cells, the mRNA expression levels of gremlin-1 and fibrillin-1 were analyzed by quantitative RT-PCR. The levels were normalized to the expression levels of TATA-binding protein and are expressed relative to each control, which was set to 1. The error bars represent s.d. ($n = 2$). (**c**) Double-immunofluorescence staining of siRNA-treated H2052 cells with gremlin-1 and fibrillin-1 antibodies. Note the lack of fibrillar gremlin-1 staining in fibrillin-1-silenced cells.

8h and i). Fibrillin-1 and -2 mRNA expression levels were also significantly reduced (Figure 8h), suggesting that gremlin-1 maintains the expression of microfibrillar genes. Further, fibronectin expression was downregulated (Figure 8h), and the epithelial marker E-cadherin was upregulated (Figure 8j). These results suggest that EMT-related alterations are reversed in gremlin-1-silenced cells.

Slug expression and EMT-phenotype are also associated with tumor chemoresistance.[18–21] The importance of high gremlin and slug expression to sensitivity to paclitaxel-mediated mesothelioma cell death was analyzed using the MTT proliferation/viability assay. H2052 cells, which express high levels of gremlin-1 and slug, were found more resistant to paclitaxel than H2452 cells (Figure 8k). Next, control and gremlin-1 siRNA-transfected H2052 cells were treated with paclitaxel or pemetrexed, and cell numbers were quantified 3 days after transfection. Treatment with paclitaxel or pemetrexed in combination with gremlin-1 siRNA led to efficient cell death (Figure 8l).

DISCUSSION

Gremlin-1-mediated inhibition of BMP-signaling is important for normal development. Mice lacking gremlin-1 die before birth because of severe defects in kidney and lung development.[10] In

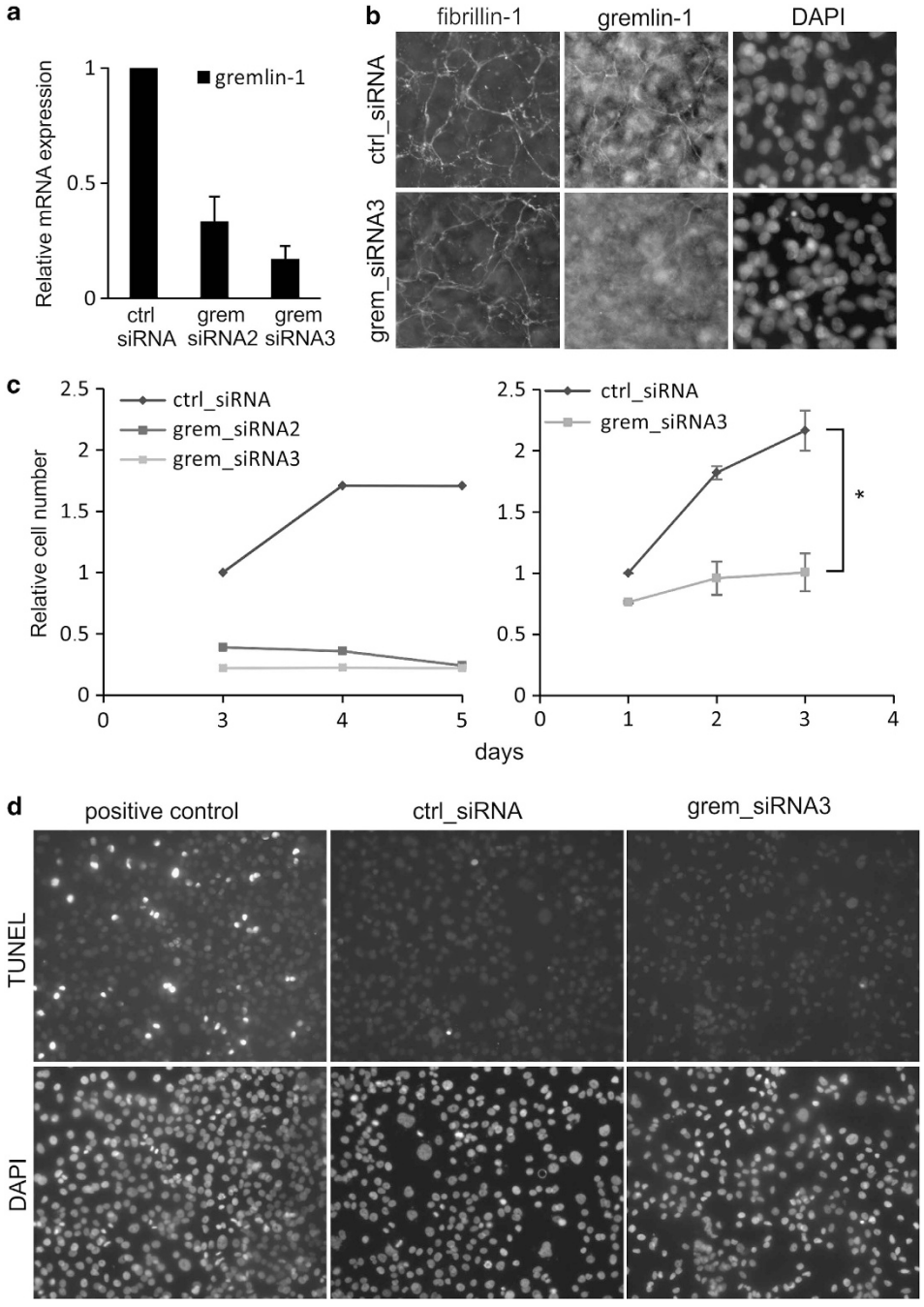

Figure 6. Gremlin-1 silencing impairs H2052 mesothelioma cell proliferation. (**a**) The efficiency of gremlin-1 siRNA silencing was analyzed with quantitative RT-PCR as in figure 5. The error bars represent s.d. ($n = 4$). (**b**) Double immunofluorescence staining of siRNA-treated H2052 cells with gremlin-1 and fibrillin-1 antibodies. Note the lack of fibrillar gremlin-1 staining, which is suggestive of efficient silencing using gremlin siRNA3. (**c**) H2052 cell proliferation was analyzed by counting cells 1–5 days after siRNA transfection. Both gremlin siRNAs reduced dramatically the number of cells 3–5 days after transfection (left panel, a representative experiment is shown). Same effect was seen also at earlier time points (right panel). The error bars represent s.d. ($n = 3$, $^*P = 0.05$). (**d**) Silencing gremlin-1 by siRNA3 did not induce apoptosis as measured using TUNEL staining. DNase I-treated cells (control) show positive staining. Nuclei are stained with DAPI.

adult tissues including lung gremlin-1 expression is low. In idiopathic pulmonary fibrosis , gremlin-1 is highly upregulated in the lung parenchyma, where it contributes to idiopathic pulmonary fibrosis pathogenesis by blocking BMP-mediated signals.[16] Gremlin-1 has been found to be upregulated also in many carcinoma tissues as well as in mesothelioma.[12,13,22] The role of gremlin-1 in malignant tissue appears complex and is likely mediated both by BMP-dependent and -independent functions. There are reports suggesting tumor-specific gremlin-1 expression,[12] while other reports suggest expression in cancer-associated stromal cells.[13] Here, we find high gremlin immunoreactivity in the mesothelioma tumor tissue. Analyses of serial mesothelioma tissue sections suggested that gremlin-1 can localize to calretinin-positive, epithelial-appearing tumor areas and also to aberrant looking and stromal-like calretinin-negative areas. These tissue areas contained some WT1-positive tumor cells.

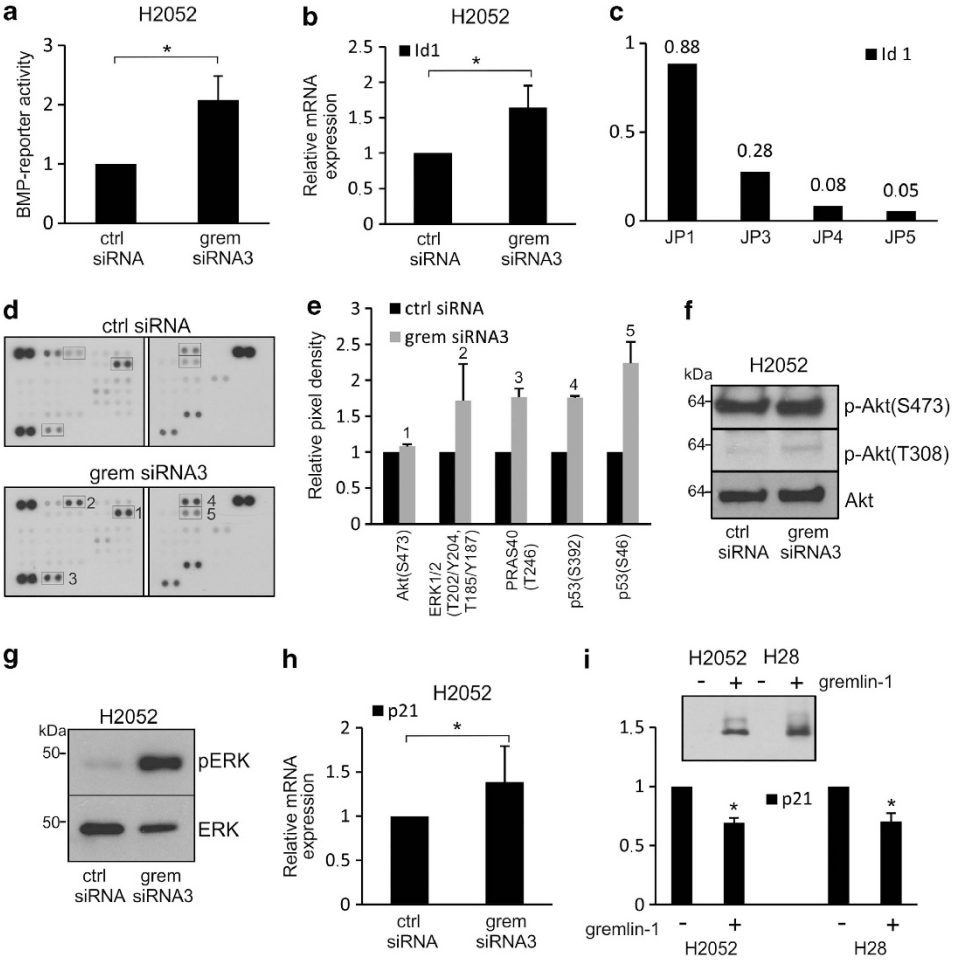

Figure 7. Cellular signaling in gremlin-1-silenced cells. (**a**) BMP-dependent reporter activity was analyzed in control and gremlin-1 siRNA-treated H2052 cells. The levels are expressed relative to control, which was set to 1. The error bars represent s.d. ($n = 4$, $^*P < 0.01$). (**b**) Id1 mRNA expression levels were analyzed by quantitative RT–PCR. The levels are expressed relative to control. $n = 3$, $^*P < 0.05$. (**c**) Id1 mRNA expression levels in primary mesothelioma cells. The levels are expressed relative to the expression levels in Met5A cells. (**d**) Cell lysates from control and gremlin-1 siRNA-treated H2052 cells were analyzed using a commercial phospho-protein array. (**e**) Quantification of alterations in the amounts of phospho-proteins ($n = 2$). Changes were also verified by immunoblotting analyses of Akt (**f**) and ERK (**g**) pathway proteins. Molecular weight markers are indicated on the left. Expression levels of p21 (Cip1/Waf1), a p53 target gene, were analyzed in gremlin-1 siRNA-treated (**h**) and gremlin-1-transfected cells (**i**) by quantitative RT-PCR. The levels are expressed relative to control, which was set to 1. $n = 3$, $^*P < 0.05$. I, inset. Gremlin-1 overexpression in H2052 and H28 cells was verified by immunoblotting using an antibody against the V5 tag.

Our results suggest that gremlin-1 localizes mainly in and around mesothelioma tumor cells.

Using a sophisticated large-scale protein interaction screen, we were able to identify fibrillin-2 as a novel gremlin-1 interacting protein. The interaction was also verified using a cell surface plasmon resonance technology. *Fibrillin-2* is a developmental gene, which is found in adult vasculature and is upregulated in idiopathic pulmonary fibrosis, scleroderma and during skin wound healing.[23,24] Idiopathic pulmonary fibrosis and cancer pathogenesis have common features including aberrant activation of mediators of tissue repair processes.[25] Our discovery that high fibrillin-2 immunoreactivity is associated with mesothelioma tumor tissue is a novel finding and supports this idea. Fibrillins (fibrillin-1 and -2) are large extracellular glycoproteins, which form heteromeric fibrillar structures, the so called fibrillin microfibrils, which are essential for elastin assembly.[26] Fibrillins also regulate growth factor signaling by sequestering TGF-β complexes as well as BMP-isoforms into extracellular matrix structures.[27] Gremlin-1 can bind to and inhibit the functions of BMP-2, -4 and -7, all of which have been shown to associate with fibrillins.[9] Here, we find that gremlin-1 can bind to fibrillin-1 and -2 *in vitro* and colocalizes with fibrillin-2 in mesothelioma tumor tissue *in vivo*. Conceptually this is a new finding, spatially localizing a BMP inhibitor molecule with its target proteins through fibrillin microfibrils. High levels of fibrillin-2 are likely to contribute to tumor cell behavior through aberrant extracellular matrix structure and regulation of gremlin-1 function.

Primary mesothelioma cells were cultured from patients' pleural effusion samples and analyzed after few passages of culture. Immunofluorescence microscopy analyses indicated that the cells, which were able to grow, represented mostly tumor cells. Gremlin-1 was expressed at mRNA and protein levels and fibrillin-2 at mRNA level by these primary cells, suggesting that they retain the pathological expression pattern of these genes. Interestingly, fibrillin-1 but not fibrillin-2 protein was detected in the matrix structures after 1 week culture of the primary cells. This likely reflects the temporal production of ECM proteins and remodeling of matrix structures during *in vitro* cell cultures.[28,29] Fibrillin-2 is likely assembled late during this process. In agreement with the protein interaction studies, gremlin-1 localized to fibrillin-1-

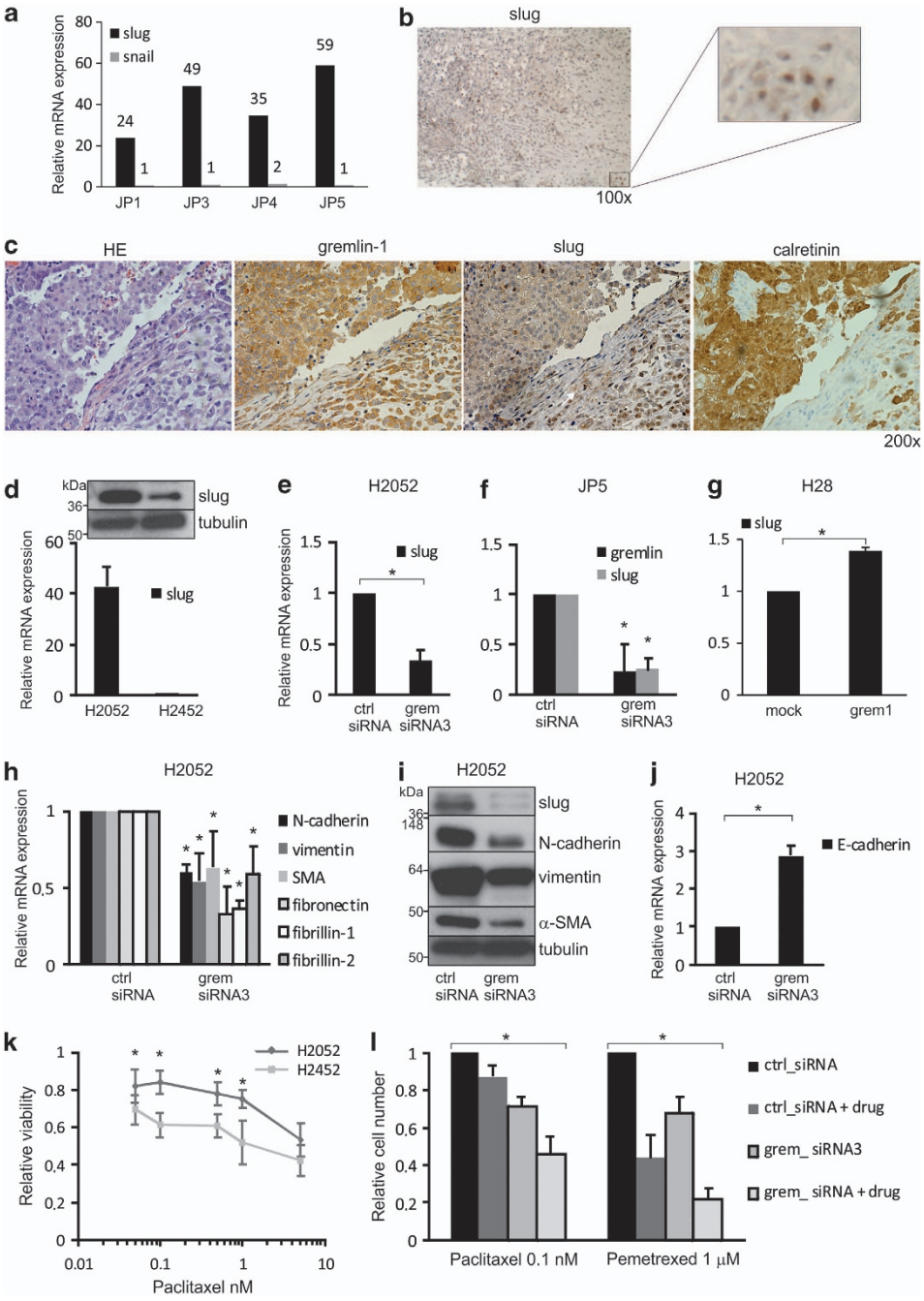

Figure 8. Gremlin-1 regulates slug expression and EMT phenotype. (**a**) Primary human mesothelioma cells (JP) were analyzed for snail and slug mRNA expression by quantitative RT-PCR. The levels were normalized to the expression levels of TATA-binding protein and are expressed relative to the expression levels in Met5A cells, which were set to 1. (**b**, **c**) Immunohistochemical staining of a mesothelioma section using slug antibodies shows mostly diffuse and granular cytoplasmic staining in the tumor tissue. Nuclear staining was also observed in certain tumor areas (**b**, right panel). (**c**) Analyses of serial mesothelioma tissue sections suggested that slug and gremlin staining colocalized in the same tumor areas. (**d**) Slug mRNA expression levels in H2052 and H2452 cells were analyzed by quantitative RT–PCR. The levels are expressed relative to H2452 expression levels, which were set to 1. The error bars represent s.d. ($n = 5$). INSET: immunoblotting analyses of slug. Tubulin is used as a loading control. Molecular weight markers are indicated on the left. (**e**–**g**) Slug mRNA expression levels were analyzed in control and gremlin-1 siRNA-treated H2052 and JP5 cells or H28 cells transfected with gremlin-1 (grem1) or control vector (mock). The levels are expressed relative to control, which was set to 1. The error bars represent s.d. (JP5, $n = 3$, $^*P < 0.05$; H2052, $n = 4$, $^*P < 0.01$; H28, $n = 3$, $^*P = < 0.05$). (**h**) N-cadherin, vimentin, α-SMA, fibronectin and fibrillin mRNA expression levels were analyzed in control and gremlin siRNA-treated H2052 cells by quantitative RT-PCR. The error bars represent s.d. ($n \geqslant 3$, $^*P < 0.05$). (**i**) Immunoblotting analyses of slug, N-cadherin, vimentin and α-SMA in control and gremlin-1 siRNA-treated H2052 cells. Tubulin is used as a loading control. (**j**) E-cadherin mRNA expression levels were analyzed in control and gremlin siRNA-treated H2052 cells by quantitative RT–PCR. Error bars represent s.d. ($n = 3$, $^*P < 0.05$). (**k**) H2052 and H2452 cells were treated with the indicated concentrations of paclitaxel after which cell proliferation/viability was analyzed with MTT assay ($n = 4$, $^*P < 0.05$). (**l**) Quantification of cell numbers after combined treatment with control or gremlin-1 siRNA and paclitaxel (0.1 nM, 24 h) or pemetrexed (1 μM, 48 h). Cell numbers were counted 3 days after transfection ($n \geqslant 4$, $^*P = 0.002$).

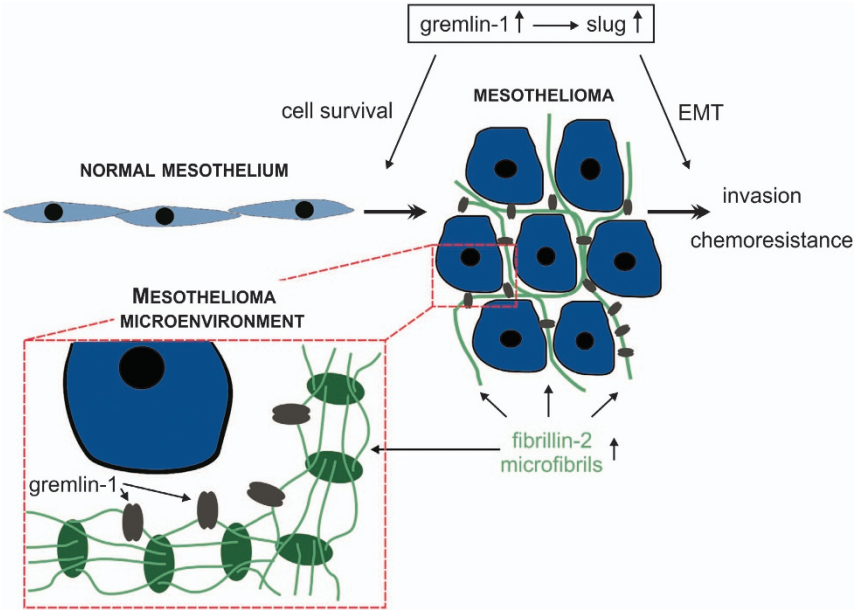

Figure 9. A model for the functions of gremlin-1 and fibrillin-2 in mesothelioma. Gremlin-1 induces proliferation and epithelial-to-mesenchymal transition (EMT) in mesothelioma cells. EMT is mediated by induction of the transcription factor slug and leads to chemoresistance and acquisition of invasive properties. Gremlin-1 is targeted to the tumor microenvironment through binding to fibrillin-2 microfibrils.

containing structures in mesothelioma cell ECM. Gene expression analyses suggested that compared with immortalized but non-tumorigenic mesothelial cells (Met5A), primary mesothelioma cells also expressed significantly higher levels of BMP-2. This is an interesting finding as BMP-2 has been linked to tumor invasion and metastasis.[30–32] Future studies will reveal whether BMP-2 is functional in the presence of high levels of its inhibitor protein.

We used the knowledge of gene expression patterns of primary mesothelioma cells to find a representative established mesothelioma cell line for mechanistic studies. H2052 cells expressed high levels of gremlin-1, fibrillin-2 and BMP-2 similar to all of the primary cells. Gremlin-1 silencing in these cells reduced cell proliferation dramatically. This is in agreement with previous studies suggesting that gremlin-1 can induce proliferation of cancer cells.[33–35] Interestingly, we observed gremlin-1 immunoreactivity also in reactive mesothelium, which associates gremlin-1 expression to a proliferative phenotype even in non-malignant mesothelial cells. Gremlin-1 expression has been linked to mesenchymal cells surrounding stem cell niches, which support proliferation of epithelial cells through blocking BMP activities.[13,36] Mesenchymal stem cells also express high levels of gremlin-1 (GeneSapiens database[37]). Our data suggest a model in which cancer cells can acquire the ability to produce high levels of gremlin-1, which is targeted to the tumor microenvironment through fibrillin binding (see Figure 9).

Signaling pathways linked to the regulation of cell survival, apoptosis and autophagy were altered in gremlin-1-silenced H2052 cells. Similar to our findings, negative regulation of Erk1/2 phosphorylation by gremlin-1 has been previously found in osteosarcoma cells;[38] however, gremlin overexpression in Saos-2 cell was found to reduce proliferation. We observed increased p53 phosphorylation and expression of its target gene, *p21*, in gremlin-1-silenced cells, suggesting a link to reduced cell survival. Further, the phosphorylation of the Akt substrate PRAS40 was significantly increased. Although PRAS40 has been linked to diabetes and cancer, its pathological functions are not well understood.[39] Interestingly, gremlin-1 has been shown to bind directly to a 14-3-3 protein,[12] which in turn binds and regulates the PRAS40 and other Akt/mTOR pathway proteins. Future studies will reveal the mechanistic details how cellular and secreted gremlin-1 regulates these pathways.

We and others have previously linked gremlin-1 expression to EMT processes.[16,40,41] In cancer cells, markers of EMT often suggest more advanced disease, invasive capacity and chemoresistance.[21,42] We found that the transcription factor slug, a master regulator of EMT, was upregulated in mesothelioma cells concurrently with gremlin-1. Silencing of gremlin-1 expression led to reduced slug mRNA and protein levels. Further, mesenchymal markers of EMT, vimentin, α-smooth muscle actin, fibronectin and N-cadherin were downregulated in gremlin-1-silenced cells, whereas epithelial marker E-cadherin was upregulated. These results are in agreement with previous studies linking the expression of EMT-related transcription factors to mesothelioma[43,44] and provide evidence that gremlin functions as a regulator of these transitional processes. EMT and slug expression have also been suggested to be involved in regulating cancer stemness as well as chemoresistance.[18,20,42] In agreement, we observed that high gremlin-1 and slug expressions in mesothelioma cells were associated with reduced sensitivity to paclitaxel-mediated cell death. Combined treatment with paclitaxel and gremlin-1 siRNA led to efficient cell death *in vitro*. Similar results were obtained with pemetrexed, which is a relatively new cancer drug used in the treatment of mesothelioma in combination with platinum compounds.[45] This indicates that blocking gremlin-1 function may be beneficial in mesothelioma especially when combined with chemotherapy.

Mesothelioma is an aggressive tumor with limited treatment options. Further, an increase is expected in the incidence of mesothelioma,[3,4] which sets an urgent need for new drug target molecules. Although the number of patient tissues analyzed in our study was relatively small ($n = 6$), the pathological expression of gremlin-1 was a clear concept. It is also reinforced by other studies suggesting a role for gremlin-1 in cancer cell proliferation.[12,13,33,34] Gremlin-1 has also BMP-independent angiogenic functions,[46] which may well contribute to tumor progression. Blocking gremlin-1 function in mesothelioma might offer means to fight the chemoresistance of this tumor.

MATERIALS AND METHODS

Antibodies

Antibodies used in the study are summarized in Table 2.

Patients and tissues specimen

A statement for the use of human tissue and pleural effusion materials was received from the Ethics Committee of the Helsinki University Hospital, Helsinki, Finland (number 308/13/0301/2010). All patients gave informed consent to participate in the study. Tissue biopsies and pleural effusion samples were obtained from patients undergoing diagnostic procedures and had a clinical and/or radiological suspicion of malignant mesothelioma. All patients included in the study ($n = 7$) were later diagnosed to have mesothelioma (Table 3). Control pleural samples were obtained from two male smokers who were operated for pneumothorax.

Cell culture and transient transfection

Immortalized normal mesothelial cells (Met5A),[47] and mesothelioma cell lines (211H, H28, H2452 and H2052) were from ATCC. Primary mesothelioma cells (named JP cells) were acquired from pleural effusion samples from patients suffering from malignant mesothelioma. Cells were centrifuged, washed and seeded on plastic culture dishes in RPMI-1640 medium (Sigma, St Louis, MO, USA) supplemented with 10% fetal bovine serum (Sigma) and antibiotics. The medium was changed every 3–4 days. Cells were passaged 2–3 times before immunofluorescence analysis of mesothelioma marker proteins was performed. Cells were also cultured for 6–7 days for RNA isolation and gene expression analyses. For further experiments JP5 cells were cultured and used between passages 3–7. Transfection of cells was carried out using siRNAs for gremlin, fibrillin-1 or a negative control (Life Technologies, Paisley, UK) as described.[48] The BMP reporter construct (Bre2-luc, kindly provided by Dr Peter ten Dijke, Leiden University Medical Center, the Netherlands) was transfected into H2052 cells to assess BMP-dependent signaling activity as described.[49]

Expression constructs and stable transfection

C-terminal gremlin-1 construct was generated by Gateway-cloning, the gremlin-1 construct from the Human Orfeome Collection (Thermo Scientific, FL, USA) to a pTO-SHc-GW-FRT plasmid with c-terminal Strep-tag III and human influenza hemagglutinin (HA)-tag.[14] Flip-In human embryonic kidney (HEK) 293 cells (Life Technologies) were grown as recommended. Stable transfection of cells was carried out as described.[50] After 2 weeks of culture, hygromycin B-resistant clones were tested for tetracycline (Sigma)-inducible gremlin-1 expression (see Figure 1b).

Affinity purification

Transfected Flip-In HEK293 cells were stimulated with tetracycline (25 ng/ml) to induce gremlin-1 expression. After a 24-h stimulation, cells were lysed in HNN-lysis buffer (50 mM HEPES pH 8, 150 mM NaCl, 50 mM NaF, 1 mM PMSF, 1.5 mM Na-vanadate, 0.5% NP-40 and protease inhibitors (Sigma)) followed by double affinity purification as described.[50] Briefly, cell lysates were passed through Strep-Tactin columns (IBA GmbH) followed by elution of bound proteins with 2.5 mM biotin. Next, the eluate was immunoprecipitated using anti-HA agarose (Sigma). Proteins were finally eluted using 0.2 M glycine and neutralized.

Protein digestion

The total protein amount from the elution fractions was precipitated using trichloroacetic acid (TCA). First, TCA was added to the elution fractions to final concentration of 25% followed by incubation for 30 min on ice. The precipitates were centrifuged, washed once with ice cold 0.1 M HCl in acetone and once with acetone. The pellets were then allowed to dry. For trypsin digestion the precipitated proteins were dissolved in 50 mM ammonium bicarbonate, pH 8.9, containing 0.1% Rapigest detergent (Waters, Milford, MA, USA). Proteins were reduced using DTT for 30 min at 60 °C followed by alkylation using iodoacetamide for 30 min at room temperature in dark. Proteins were digested with trypsin (Promega, Madison, WI, USA) for 18 h at 37 °C, and then the Rapigest detergent was hydrolyzed with HCl for 45 min at 37 °C. Peptides were purified with PepClean C18 Spin Columns (Thermo Fisher, Rockford, IL, USA) according to the manufacturer's protocol. Finally, the purified peptides were dissolved in 0.1% formic acid for MS analysis.

Table 3. Mesothelioma patient characteristics

Patient	*Type*	*Location*	*Age*	*Gender*	*IHC*	*Cells*
JP1	Epithelial	Pleura	53	Male	+	+
JP2	Biphasic	Pleura	71	Male	+	−
JP3	Epithelial	Pleura	63	Male	+	+
JP4	Biphasic	Peritoneum	72	Female	−	+
JP5	Epithelial	Pleura	69	Female	+	+
JP6	Biphasic	Pleura	71	Female	+	−
JP7	Epithelial	Pleura	61	Male	+	−

Tissues analyzed by immunohistochemistry (IHC) and pleural effusion samples obtained for cell culture (cells) are indicated.

Table 2. List of antibodies used in the study

Name	*Source*	*Application*	*Supplier*
calretinin	mouse/DAK-Calret1	IF, IHC	DAKO, Glostrup, Denmark, Germany
cytokeratin-7	rabbit /EP16204	IF	Novus Biologicals, Littleton, CO, USA
vimentin	mouse/V9	IF, IB	Santa Cruz, Santa Cruz, CA, USA
N-cadherin	mouse/32	IB	BD Biosciences, Franklin Lakes, NJ, USA
α-SMA	mouse/1A4	IB	Sigma, St Louis, MO, USA
HA	mouse/16B12	IB	Covance, Princeton, NJ, USA
fibrillin-1	mouse/2499	IF	Millipore, Billerica, MA, USA
fibrillin-1	rabbit/ pAb9543	IHC, IF	Professor Lynn Sakai
fibrillin-2	mouse/48	IHC, PLA	Millipore
gremlin-1	rabbit pAb	IHC	Abcam, Cambridge, UK
gremlin-1	goat pAb	IHC, PLA	Santa Cruz
gremlin-1	rabbit pAb	IF	Santa Cruz
Slug	rabbit pAb	IB, IHC	Sigma
WT1	mouse/WT49	IHC	Novocastra, Newcastle, UK
p-Akt (S473)	rabbit pAb	IB	Cell Signaling, Danvers, MA, USA
p-Akt (T308)	rabbit pAb	IB	Cell Signaling
Akt	rabbit pAb	IB	Cell Signaling
p-Erk1/2	rabbit mAb/D13.14.4E	IB	Cell Signaling
Erk1	mouse/3A7	IB	Cell Signaling
V5	Mouse mAb	IB	Invitrogen

Abbreviations: IB, immunoblotting; IF, immunofluorescence; IHC, immunohistochemistry; PLA, proximity ligation assay.

LC-MS/MS analysis

Mass spectrometric analysis was performed using nanoAcquity UPLC – liquid chromatography system on-line with a Waters Synapt G2 mass spectrometer (Waters S.A.S., Saint-Quentin, France). Waters nanoAcquity UPLC Trap Column (Symmetry C18, 180 μm × 20 mm, 5 μm) was used as trapping and Waters nanoAcquity UPLC Column (BEH130 C18, 75 μm × 150 mm, 1.7 μm) as analytical column. Four microliters of sample was injected and run using 90 min gradient from 3 to 40% mobile phase B (0.1% formic acid in acetonitrile). 0.1% formic acid in water was used as mobile phase A.

Data were collected with data dependent acquisition manner collecting eight fragmentation spectra simultaneously. Switch limit from MS to MS/MS was set to peak intensity of 200. Fragmentation data for detected peaks were collected for 5 s and then excluded from fragmentation for 120 s. Scan time for both MS and MS/MS was one second. No lockmass correction was used.

The raw data were processed with Mascot Distiller software (version 2.3.1.0, Matrix Science, London, UK), and database search was performed using Mascot search engine (version 2.2.04) against Swiss-Prot human database (dated 16.6.2010). MudPIT scoring and Ion score cutoff limit of 20 were used to identify peptides. Require bold red- specification was used to limit the results to those proteins that have at least one unique peptide. Carbamidomethylated cysteine was set as fixed modification and oxidation of methionine as variable modification. Peptide mass tolerance for search was 0.2 Da and 0.1 Da for fragment ion search. A maximum of two missed trypsin cleavages was allowed. The Mascot Distiller processed data were also searched using GPM X!Tandem search engine[51] using same parameters.

Expression and purification of recombinant gremlin-1

The expression construct pGremlin-1_V5/HIS in pEF-IRES-P contains cDNA encoding human gremlin-1 with C-terminal tags (V5 and 6HIS). H2052 and H28 cells were transiently transfected with this construct or the expression vector using Fugene HD transfection reagent (Promega). CHO cells were stably transfected, and gremlin-containing cell culture supernatants were produced as described.[52] The media was then dialyzed against 50 mM sodium phosphate buffer, pH 7.2 and 1 M NaCl (buffer A) and loaded on a 1-ml HiTrap column (GE Health Care, Waukesha, WI, USA) previously charged with $CoCl_2$ and equilibrated with buffer A. The loaded column was washed with 40 column volumes of buffer A and subjected to a fast protein liquid chromatography (GEHC) gradient run starting with buffer A containing 0–100% buffer B (buffer A with 250 mM imidazole). Fractions were analyzed using SDS–PAGE for their purity and molecular mass, and imidazole in these fractions was removed by dialysis against buffer A. For further concentration and purification, gremlin-1-containing fractions were dialyzed against TBS and subjected to affinity chromatography using a 1-ml HiTrap heparin column (GEHC). Bound gremlin-1 was eluted in a 0–1 M NaCl gradient.

Surface plasmon resonance

Binding analyses were performed using a BIAcore2000 (GEHC). 2000 Rus of gremlin-1 were covalently coupled to carboxymethyldextran hydrogel 500 M sensor chips (XanTec, Düsseldorf, Germany) using the amine coupling kit following the manufacturer's instructions (GEHC). Binding assays with N-terminal fibrillin-1 (rF11) and -2 peptides (rF86) as analytes were performed as previously described.[9] Kinetic constants were calculated by nonlinear fitting of association and dissociation curves (BIAevaluation 4.1 software).

Immunohistochemical staining and proximity ligation assay

Immunohistochemical staining of tumor tissues and proximity ligation assay were performed as described.[24] Images were captured with Nikon DS-Fi1 or with Axio Imager with ApoTome (Zeiss, Göttingen, Germany) or with using Axio Vison 4.8 software (Zeiss).

SDS–PAGE and immunoblotting

Cells were lysed in RIPA lysis buffer (50 mM Tris-HCl, pH 7.4, 150 mM NaCl, 1 mM EDTA, 1% NP-40, 0.2% sodium deoxycholate) containing protease inhibitors (Roche, Mannheim, Germany) for 15 min on ice. Protein concentrations were measured using a BCA protein assay Kit (Pierce, Rockfors, IL, USA). SDS–PAGE and immunoblotting were performed as described.[53]

RNA isolation and gene expression analyses

Isolation of total cellular RNA, reverse transcription and quantitative real-time PCR were carried out as described.[53] The relative gene expression differences were calculated with the comparative delta delta cycle threshold (ΔΔCT) method, and the results have been expressed as mRNA expression levels normalized to the levels of a gene with a constant expression (TATA-binding protein).

Immunofluorescence analyses and microscopy

Cells were grown on glass coverslips for the indicated times and fixed with 4% paraformaldehyde in PBS at room temperature for 10 min or with ice cold methanol at $-20\,^{\circ}C$ for 20 min. Immunofluorescence staining was carried out as described.[53] Images were captured with a Axioplan 2 epifluorescence microscope (Zeiss) and AxioCam HRm 14-bit grayscale CCD camera Axiovision 4.6 software (Zeiss).

Human phospho-kinase array

Control and gremlin-1 siRNA-treated cells were lysed, and alterations in phospho-kinase levels were analyzed using a Proteome profiler array (ARY003b, R&D Systems, Gaitherburg, MD, USA) according to the manufacturer's instructions. Quantity One version 4.6 (BioRad, Hercules, CA, USA) was used for quantification. The kinase array was performed twice, and the results are expressed as average of the two experiments.

Measurements of cell viability and apoptosis

Cell proliferation/viability was assessed using MTT assay (R&D Systems). Briefly, cells were seeded on 96-well plates (10 000/well) and were treated the next day with different concentrations of paclitaxel (Hospira, Lake Forest, IL, USA). The metabolic activity of cells was measured after 48 h according to the manufacturer's instructions. Apoptosis was assayed using a TUNEL technology using *In Situ* cell death detection kit (Roche). Cells were seeded on glass coverslips, cultured overnight and transfected with siRNAs. Cells were then fixed and stained, according to the manufacturer's instructions, 3 days after transfection.

Statistical analyses

Data were analyzed using PASW Statistics 18 program for Windows (SPSS, Chicago, IL, USA). Statistical difference between two independent groups was evaluated using nonparametric Mann–Whitney *U*-test. Statistical difference between more than two independent groups was evaluated using nonparametric Kruskal–Wallis test. A *P*-value of <0.05 was considered statistically significant.

CONFLICT OF INTEREST

The authors declare no conflict of interest.

ACKNOWLEDGEMENTS

We thank Eva Sutinen for coordinating patient sample collection and performing immunohistochemical staining experiments, Arja Pasternack for CHO cell transfection and production of conditioned media, Sami Starast for technical assistance, Professor Jorma Keski-Oja for discussions, Professor Lynn Sakai (Oregon Health and Science University, Portland, OR) for the fibrillin-1 antibody and fibrillin-1 and -2 peptides, and Biomedicum Imaging Unit for imaging support. This work was supported by Academy of Finland, Sigrid Jusélius Foundation, Jalmari and Rauha Ahokas Foundation, Magnus Ehrnrooth Foundation, Finnish Cultural Foundation, Foundation of the Finnish Anti-Tuberculosis Association, Deutsche Forschungsgemeinschaft (SFB829, project B12 to GS).

REFERENCES

1 Mossman BT, Bignon J, Corn M, Seaton A, Gee JB. Asbestos: scientific developments and implications for public policy. *Science* 1990; **247**: 294–301.
2 Lanphear BP, Buncher CR. Latent period for malignant mesothelioma of occupational origin. *J Occup Med* 1992; **34**: 718–721.
3 Huuskonen MS, Rantanen J. Finnish Institute of Occupational Health (FIOH): prevention and detection of asbestos-related diseases, 1987-2005. *Am J Ind Med* 2006; **49**: 215–220.
4 Vorobiof DA, Mafafo K. Malignant pleural mesothelioma: medical treatment update. *Clin Lung Cancer* 2009; **10**: 112–117.

5 Dormoy V, Jacqmin D, Lang H, Massfelder T. From development to cancer: lessons from the kidney to uncover new therapeutic targets. *Anticancer Res* 2012; **32**: 3609–3617.
6 Micalizzi DS, Farabaugh SM, Ford HL. Epithelial-mesenchymal transition in cancer: parallels between normal development and tumor progression. *J Mammary Gland Biol Neoplasia* 2010; **15**: 117–134.
7 Hsu DR, Economides AN, Wang X, Eimon PM, Harland RM. The Xenopus dorsalizing factor Gremlin identifies a novel family of secreted proteins that antagonize BMP activities. *Mol Cell* 1998; **1**: 673–683.
8 Topol LZ, Bardot B, Zhang Q, Resau J, Huillard E, Marx M *et al.* Biosynthesis, post-translation modification, and functional characterization of Drm/Gremlin. *J Biol Chem* 2000; **275**: 8785–8793.
9 Sengle G, Charbonneau NL, Ono RN, Sasaki T, Alvarez J, Keene DR *et al.* Targeting of bone morphogenetic protein growth factor complexes to fibrillin. *J Biol Chem* 2008; **283**: 13874–13888.
10 Michos O, Panman L, Vintersten K, Beier K, Zeller R, Zuniga A *et al.* antagonism induces the epithelial-mesenchymal feedback signaling controlling metanephric kidney and limb organogenesis. *Development* 2004; **131**: 3401–3410.
11 Topol LZ, Marx M, Laugier D, Bogdanova NN, Boubnov NV, Clausen PA *et al.* Identification of drm, a novel gene whose expression is suppressed in transformed cells and which can inhibit growth of normal but not transformed cells in culture. *Mol Cell Biol* 1997; **17**: 4801–4810.
12 Namkoong H, Shin SM, Kim HK, Ha SA, Cho GW, Hur SY *et al.* The bone morphogenetic protein antagonist gremlin 1 is overexpressed in human cancers and interacts with YWHAH protein. *BMC Cancer* 2006; **6**: 74.
13 Sneddon JB, Zhen HH, Montgomery K, van de Rijn M, Tward AD, West R *et al.* Bone morphogenetic protein antagonist gremlin 1 is widely expressed by cancer-associated stromal cells and can promote tumor cell proliferation. *Proc Natl Acad Sci USA* 2006; **103**: 14842–14847.
14 Varjosalo M, Sacco R, Stukalov A, van Drogen A, Planyavsky M, Hauri S *et al.* Interlaboratory reproducibility of large-scale human protein-complex analysis by standardized AP-MS. *Nat Methods* 2013; **10**: 307–314.
15 Ramirez F, Sakai LY. Biogenesis and function of fibrillin assemblies. *Cell Tissue Res* 2010; **339**: 71–82.
16 Koli K, Myllärniemi M, Vuorinen K, Salmenkivi K, Ryynänen MJ, Kinnula VL *et al.* Bone morphogenetic protein-4 inhibitor gremlin is overexpressed in idiopathic pulmonary fibrosis. *Am J Pathol* 2006; **169**: 61–71.
17 Thiery JP, Acloque H, Huang RY, Nieto MA. Epithelial-mesenchymal transitions in development and disease. *Cell* 2009; **139**: 871–890.
18 Catalano A, Rodilossi S, Rippo MR, Caprari P, Procopio A. Induction of stem cell factor/c-Kit/slug signal transduction in multidrug-resistant malignant mesothelioma cells. *J Biol Chem* 2004; **279**: 46706–46714.
19 Haslehurst AM, Koti M, Dharsee M, Nuin P, Evans K, Geraci J *et al.* EMT transcription factors snail and slug directly contribute to cisplatin resistance in ovarian cancer. *BMC Cancer* 2012; **12**: 91.
20 Mani SA, Guo W, Liao MJ, Eaton EN, Ayyanan A, Zhou AY *et al.* The epithelial-mesenchymal transition generates cells with properties of stem cells. *Cell* 2008; **133**: 704–715.
21 Polyak K, Weinberg RA. Transitions between epithelial and mesenchymal states: acquisition of malignant and stem cell traits. *Nat Rev Cancer* 2009; **9**: 265–273.
22 Wang DJ, Zhi XY, Zhang SC, Jiang M, Liu P, Han XP *et al.* The bone morphogenetic protein antagonist Gremlin is overexpressed in human malignant mesothelioma. *Oncol Rep* 2012; **27**: 58–64.
23 Brinckmann J, Hunzelmann N, Kahle B, Rohwedel J, Kramer J, Gibson MA *et al.* Enhanced fibrillin-2 expression is a general feature of wound healing and sclerosis: potential alteration of cell attachment and storage of TGF-β. *Lab Invest* 2010; **90**: 739–752.
24 Leppäranta O, Sens C, Salmenkivi K, Kinnula VL, Keski-Oja J, Myllärniemi M *et al.* Regulation of TGF-β storage and activation in the human idiopathic pulmonary fibrosis lung. *Cell Tissue Res* 2012; **348**: 491–503.
25 Vancheri C, Failla M, Crimi N, Raghu G. Idiopathic pulmonary fibrosis: a disease with similarities and links to cancer biology. *Eur Respir J* 2010; **35**: 496–504.
26 Lin G, Tiedemann K, Vollbrandt T, Peters H, Batge B, Brinckmann J *et al.* Homo- and heterotypic fibrillin-1 and -2 interactions constitute the basis for the assembly of microfibrils. *J Biol Chem* 2002; **277**: 50795–50804.
27 Ramirez F, Rifkin DB. Extracellular microfibrils: contextual platforms for TGFβ and BMP signaling. *Curr Opin Cell Biol* 2009; **21**: 616–622.
28 Dallas SL, Chen Q, Sivakumar P. Dynamics of assembly and reorganization of extracellular matrix proteins. *Curr Top Dev Biol* 2006; **75**: 1–24.
29 Koli K, Hyytiäinen M, Ryynänen MJ, Keski-Oja J. Sequential deposition of latent TGF-β binding proteins (LTBPs) during formation of the extracellular matrix in human lung fibroblasts. *Exp Cell Res* 2005; **310**: 370–382.
30 Gordon KJ, Kirkbride KC, How T, Blobe GC. Bone morphogenetic proteins induce pancreatic cancer cell invasiveness through a Smad1-dependent mechanism that involves matrix metalloproteinase-2. *Carcinogenesis* 2009; **30**: 238–248.
31 Kang MH, Oh SC, Lee HJ, Kang HN, Kim JL, Kim JS *et al.* Metastatic function of BMP-2 in gastric cancer cells: the role of PI3K/AKT, MAPK, the NF-κB pathway, and MMP-9 expression. *Exp Cell Res* 2011; **317**: 1746–1762.
32 Katsuno Y, Hanyu A, Kanda H, Ishikawa Y, Akiyama F, Iwase T *et al.* Bone morphogenetic protein signaling enhances invasion and bone metastasis of breast cancer cells through Smad pathway. *Oncogene* 2008; **27**: 6322–6333.
33 Kim M, Yoon S, Lee S, Ha SA, Kim HK, Kim JW *et al.* Gremlin-1 induces BMP-independent tumor cell proliferation, migration, and invasion. *PLoS One* 2012; **7**: e35100.
34 Mulvihill MS, Kwon YW, Lee S, Fang LT, Choi H, Ray R *et al.* Gremlin is over-expressed in lung adenocarcinoma and increases cell growth and proliferation in normal lung cells. *PLoS One* 2012; **7**: e42264.
35 Sneddon JB, Werb Z. Location, location, location: the cancer stem cell niche. *Cell Stem Cell* 2007; **1**: 607–611.
36 Kosinski C, Li VS, Chan AS, Zhang J, Ho C, Tsui WY *et al.* Gene expression patterns of human colon tops and basal crypts and BMP antagonists as intestinal stem cell niche factors. *Proc Natl Acad Sci USA* 2007; **104**: 15418–15423.
37 Kilpinen S, Autio R, Ojala K, Iljin K, Bucher E, Sara H *et al.* Systematic bioinformatic analysis of expression levels of 17,330 human genes across 9,783 samples from 175 types of healthy and pathological tissues. *Genome Biol* 2008; **9**: R139.
38 Chen B, Athanasiou M, Gu Q, Blair DG. Drm/Gremlin transcriptionally activates p21(Cip1) via a novel mechanism and inhibits neoplastic transformation. *Biochem Biophys Res Commun* 2002; **295**: 1135–1141.
39 Wang H, Zhang Q, Wen Q, Zheng Y, Lazarovici P, Jiang H *et al.* Proline-rich Akt substrate of 40kDa (PRAS40): a novel downstream target of PI3k/Akt signaling pathway. *Cell Signal* 2012; **24**: 17–24.
40 Carvajal G, Droguett A, Burgos ME, Aros C, Ardiles L, Flores C *et al.* Gremlin: a novel mediator of epithelial mesenchymal transition and fibrosis in chronic allograft nephropathy. *Transplant Proc* 2008; **40**: 734–739.
41 Lee H, O'Meara SJ, O'Brien C, Kane R. The role of gremlin, a BMP antagonist, and epithelial-to-mesenchymal transition in proliferative vitreoretinopathy. *Invest Ophthalmol Vis Sci* 2007; **48**: 4291–4299.
42 Shih JY, Yang PC. The EMT regulator slug and lung carcinogenesis. *Carcinogenesis* 2011; **32**: 1299–1304.
43 Fassina A, Cappellesso R, Guzzardo V, Dalla Via L, Piccolo S, Ventura L *et al.* Epithelial-mesenchymal transition in malignant mesothelioma. *Mod Pathol* 2012; **25**: 86–99.
44 Merikallio H, Pääkko P, Salmenkivi K, Kinnula V, Harju T, Soini Y. Expression of snail, twist, and Zeb1 in malignant mesothelioma. *APMIS* 2012; **121**: 1–10.
45 Pasello G, Ceresoli GL, Favaretto A. An overview of neoadjuvant chemotherapy in the multimodality treatment of malignant pleural mesothelioma. *Cancer Treat Rev* 2013; **39**: 10–17.
46 Mitola S, Ravelli C, Moroni E, Salvi V, Leali D, Ballmer-Hofer K *et al.* Gremlin is a novel agonist of the major proangiogenic receptor VEGFR2. *Blood* 2010; **116**: 3677–3680.
47 Ke Y, Reddel RR, Gerwin BI, Reddel HK, Somers AN, McMenamin MG *et al.* Establishment of a human in vitro mesothelial cell model system for investigating mechanisms of asbestos-induced mesothelioma. *Am J Pathol* 1989; **134**: 979–991.
48 Koli K, Ryynänen MJ, Keski-Oja J. Latent TGF-β binding proteins (LTBPs)-1 and -3 coordinate proliferation and osteogenic differentiation of human mesenchymal stem cells. *Bone* 2008; **43**: 679–688.
49 Myllärniemi M, Lindholm P, Ryynänen MJ, Kliment CR, Salmenkivi K, Keski-Oja J *et al.* Gremlin-mediated decrease in bone morphogenetic protein signaling promotes pulmonary fibrosis. *Am J Respir Crit Care Med* 2008; **177**: 321–329.
50 Glatter T, Wepf A, Aebersold R, Gstaiger M. An integrated workflow for charting the human interaction proteome: insights into the PP2A system. *Mol Syst Biol* 2009; **5**: 237.
51 Fenyo D, Eriksson J, Beavis R. Mass spectrometric protein identification using the global proteome machine. *Methods Mol Biol* 2010; **673**: 189–202.
52 Hulmi JJ, Oliveira BM, Silvennoinen M, Hoogaars WM, Ma H, Pierre P *et al.* Muscle protein synthesis, mTORC1/MAPK/Hippo signaling, and capillary density are altered by blocking of myostatin and activins. *Am J Physiol Endocrinol Metab* 2013; **304**: E41–E50.
53 Tamminen JA, Myllärniemi M, Hyytiäinen M, Keski-Oja J, Koli K. Asbestos exposure induces alveolar epithelial cell plasticity through MAPK/Erk signaling. *J Cell Biochem* 2012; **113**: 2234–2247.